https://www.sciencedirect.com/science/article/abs/pii/S0278612517300328

DOI: 10.1016/j.jmsy.2017.03.003

Milan, 21/02/2017

Hermes Giberti
Luca Sbaglia
Marcello Urgo

Highlights

Following are the main points of the article.

Introduction An introduction is given on the importance of the path planning field in manufacturing processes with a main focus on extrusion systems.

Extrusion systems The article is focused on extrusion systems as painting, gluing and AM FDM techniques. Typical path planning algorithm are described outlining the importance of a uniform distribution of material in order to obtain high quality products.

Path planning algorithm Starting from a curve parameterization desired is described a path planning algorithm based on the use of Bézier curve by aiming to achieve a constant velocity with a TCP, tool center point. The algorithm is based on the use of straight and parabolic lines. A possibility to extend the algorithm through the use of weights is described.

Actual application An actual example is made through the use of a real AM, additive manufacturing, machine. It's shown the feasibility of the algorithm with the possibility to take into account the dynamic of a specific process. The same algorithm could be tailored on a different machine.

H.Giberti, L.Sbaglia, M.Urgo

A path planning algorithm for industrial processes under velocity constraints with an application to additive manufacturing

Hermes Giberti[a], Luca Sbaglia[b], Marcello Urgo[c]

[a] Università degli Studi di Pavia, Dipartimento di Ingegneria Industriale e dell'Informazione, Via A. Ferrata 5, 27100 Pavia, Italy
[b] Università degli Studi di Parma, Industrial Engineering Department, Via delle Scienze 181/A, 43124 Parma, Italy
[c] Politecnico di Milano, Mechanical Department, via la Masa 1, 20156 Milano, Italy

Abstract

In the operation of a broad range of industrial processes, the use of robots whose trajectories are constrained by the velocity of the parts actuated (tools, end effectors, joints and the like) more often than not play a significant role. Keeping our focus on systems for material deposition such as painting, gluing, aerosol spraying but nowadays also additive manufacturing techniques like FDM processes, it is noticeable that a key parameter is the control of the flow of material in accordance with the trajectory velocity of the parts being actuated.

According to the specific requirements and goals of different technology, it is possible to generate different trajectories. In this paper, we propose an original path planning algorithm based on the use of Bezier curves aimed at assuring regulation of the velocity and a uniform distribution of the extruded material referring to an innovative additive manufacturing technology.

In particular, the paper presents a path planning technology developed for an application where it is necessary to maintain a constant velocity along the length of the trajectory aimed at improving the technological processes on the basis of an innovative additive technology.

Email addresses: hermes.giberti@unipv.it (Hermes Giberti), luca.sbaglia@studenti.unipr.it (Luca Sbaglia), marcello.urgo@polimi.it (Marcello Urgo)

The paper further presents a working application with a machine prototype so as to demonstrate the viability and performance of the work under consideration.
Keywords: path planning algorithm, Bézier curves, additive manufacturing, constant feed rate, constant extrusion rate,

---

1. Introduction and Problem Statement

The field of path planning has been widely studied in robotics aimed at defining the trajectory and the movement of the end-effector in a robot workspace. The role of path planning in industrial processes has been further increased to also take into consideration process planning i.e., how to control a process in terms of movement and technological parameters in order to achieve the required result. Further developments in this field are also due to the robot adoption into the additive manufacturing as the result of continuously growing technology capable of processing new shapes and materials.

The aim of this article is to propose a path-planning algorithm to ensure an even material distribution in a specific range of industrial processes, e.g., painting, gluing, aerosol spraying and additive manufacturing processes. A specific focus is given to extrusion systems where the extrusion rate cannot be adequately controlled. In such cases it is necessary and in fact better to maintain the extrusion velocity constant, as is the cases set out in this article, where, for the development of an innovative AM technology, the maintaining of a constant flow rate is required.

A path-planning algorithm is proposed using Beziér curves to guarantee a proper regulation of the relative velocity between the end-effector and the part to process. Bézier curves are exploited for the generation of an interpolation of the ideal trajectory based on straight and parabolic segments. Regulating the parametric velocity along the trajectory, the original approach proposed in this paper allows the moving of tool center point (TCP), with constant and regulated velocity during virtually the whole of the trajectory. In fact some slight oscillations in the velocity are unavoidable but the proposed approach is aimed at keeping such fluctuations extremely low and controllable.

2. Literature Review

Among AM techniques the ones based on the extrusion of material, such as FDM, have been the subject of many studies in particularly after the expiry of the patent related to this technology[1] and thus making spreading the use of this technique within the market.

For instance, Roberson et al. [2] show the use of an FDM technique for new materials in the manufacture of electromechanical and electromagnetic applications, whereas Volpato et al. [3] show an innovative piston-driven extrusion head that capable of extruding polypropylene granules into a filament. Giberti et al.[4],[5], [6] show several studies on a new 3D printing solution for metal parts based on a MIM technique.

Some of these studies focus on the optimization of the technological parameters [7], or on the attempt to model particular characteristics of these processes, [8][9]. In fact, as observed by Jiang et al.[10], It is paramount to obtain a uniform-distributed material thickness for the accuracy of these processes and to characterize their behaviour.

For the reasons set out above the deposition method and the tool path generation of the AM technique must be taken into great consideration according to the different goals to be achieved. Kulkarni et al.[11] study the importance of the tool path planning on the resulting stiffness of the printed objects. Jin et al.[12][13] propose a new path planning algorithm in order to minimize the building time of the part at the same time maintaining a good surface accuracy. In order to overcome deposition problems, related to a new metal based AM technique, Mireles et al.[14] were required to modify the toolpath commands of a pre-existing FDM machine. Rishi [15] has shown how a different feed rate can be used to improve accuracy of the surface or the building time of the internal parts; whereas for systems based on a constant feed rate, in order to guarantee a uniform material deposition, the Direction-Parallel Tool-Path (DP) technique can be used to achieve this goal.

Some articles are available in literature proposing DP deposition trajectories using an approach based on lines and parabolas and moving the end-tool with constant feed rate where possible along the trajectory. Thompson [16] shows constant material flow trajectories for straight lines using a constant acceleration to link the velocity for two consecutive lines with different velocities: in this way an absolute velocity error is introduced where the smaller the angle between the two consecutive lines the greater the error. This requires the need to change the material flow during the parabolic segments.

Jin [17] suggests a straight lines and parabolas trajectory based entirely on the curvilinear abscissa velocity control. Defining two lines typologies (type I used for lines which intersect the deposition profile, and type II for lines adjacent to the profile boundaries) a different absolute velocity is imposed on the two types: usually velocity I is double velocity II and a constant acceleration profile is used to link the two lines on the curvilinear abscissa. The extruder motion profile is created taking into account the velocity variations of the control parameters. This strategy leads to limited accelerations on active joints during curved paths attaining a good printing velocity.

In the field of CNC machining the use of Bézier curves has been exploited in order to obtain continuity on the velocity and acceleration usually not obtainable by the G-Code based on straight lines and the use of G1 commands [18].

Compared to the literature referred above, the approach proposed in this paper allows the moving of tool center point (TCP), with constant and regulated velocity during virtually the whole of the trajectory assuring the possibility to extrude without changing the flow rate. Because some slight oscillations in the velocity are unavoidable, this method is aimed at keeping such fluctuations not only extremely low but also controllable and predetermined.

3. Curve Parametrization

To define a trajectory in a cartesian space (XYZ) is necessary to define a parametric geometrical path, as defined by [19]:

$$\mathbf{p} = \mathbf{p}(u), \qquad u \in [u_{min}, u_{max}] \tag{1}$$

where $\mathbf{p}(u)$ is a continuous vectorial function(3x1) which describes the path inside the workspace as a function of the independent variable u. We take into account 3 Dofs, but we can extend the definition of $\mathbf{p}$ in order to include more Dofs.

The so defined vector function is controlled imposing a motion profile on parameter $u = u(t)$ which describes the tool trajectory along its path.

in particular:

$$\left|\dot{\tilde{\mathbf{p}}}(t)\right| = v_c = constant \tag{2}$$

where $\tilde{\mathbf{p}}(t) = (\mathbf{p} \circ u)(t)$, and for velocity and acceleration we derive the last equation.

It's not needed to analytical obtain function $u(t)$, its value $u(t_k) = u_k$ can be computed with a temporal discretization $t_k = kT_s$, with T_s sample time. We can obtain u_k with $k = 0, 1, 2, ...$, using a Taylor series with a second order approximation. Deriving respect to the time the following conditions are obtained:

$$\dot{u}(t) = \frac{v_c}{\left|\frac{d\mathbf{p}}{du}\right|} \qquad \ddot{u}(t) = -v_c^2 \frac{\frac{d\mathbf{p}^T}{du} \cdot \frac{d^2\mathbf{p}}{du^2}}{\left|\frac{d\mathbf{p}}{du}\right|^4} \tag{3}$$

considering a second order approximation the variable value u at time $(k+1)T_s$

can be determined as:

$$u_{k+1} = u_k + \frac{v_c T_s}{\left|\frac{d\mathbf{p}}{du}\right|_{u_k}} - \frac{(v_c T_s)^2}{2} \left[\frac{\frac{d\mathbf{p}^T}{du} \cdot \frac{d^2\mathbf{p}}{du^2}}{\left|\frac{d\mathbf{p}}{du}\right|^4} \right]_{u_k} \tag{4}$$

In order to achieve a constant velocity trajectory in the initial and final part of the path there is a non-zero acceleration. Considering a trapezoidal velocity the computing of u_{k+1} is modified as follow:

$$u_{k+1} = u_k + \frac{v_k T_s}{\left|\frac{d\mathbf{p}}{du}\right|_{u_k}} + \frac{T_s^2}{2} \left\{ \frac{a_k}{\left|\frac{d\mathbf{p}}{du}\right|_{u_k}} - v_k^2 \left[\frac{\frac{d\mathbf{p}^T}{du} \cdot \frac{d^2\mathbf{p}}{du^2}}{\left|\frac{d\mathbf{p}}{du}\right|^4} \right]_{u_k} \right\} \tag{5}$$

where $a_k = a(t_k)$ and $v_k = v(t_k)$ are respectively acceleration and velocity at instant $t_k = k \cdot T_s$.

To define a deposition trajectory which guarantees a constant feed rate of the tool in necessary to implement a parametric curve defined in the tool workspace. In order to achieve this goal *Bézier curves*, are exploited to generate a parametric path made of straight lines and parabolas.

A *Bézier curve* of m degree is defined as:

$$\mathbf{b}(u) = \sum_{j=0}^{m} B_j^m(u)\mathbf{p}_j, \qquad 0 \le u \le 1 \tag{6}$$

where coefficients $\mathbf{p}_j$ are control points, and functions $B_j^M(u)$ are *Bernstein polynomials* defined as $B_j^m(u) = \begin{pmatrix} m \\ j \end{pmatrix} u^j(1-u)^{m-j}$.

The Binomial coefficient, for $j = 0, 1, ..., m$, defines the rows of the *Pascal* triangle. A *Bézier curve* derivative respect to variable u of m degree is still a *Bézier curve* of degree $m-1$ defined as:

$$\frac{d\mathbf{b}(u)}{du} = m \sum_{i=0}^{m-1} B_i^{m-1}(u)(\mathbf{p}_{i+1} - \mathbf{p}_\mathbf{i}) \tag{7}$$

4. Path Planning usign Bézier Curves

Straight lines and parabolas interpolation is used starting from *Bézier curves* of first and second degree. They are evaluated in the following manner:

$$\begin{aligned} \mathbf{b}(u) &= (1-u)\mathbf{p}_{j-1}^{u} + u\mathbf{p}_{j}^{e} && \textit{line} \\ \mathbf{b}(u) &= (1-u)^2\mathbf{p}_{j}^{e} + 2u(1-u)\mathbf{p}_j + u^2\mathbf{p}_{j}^{u} && \textit{parabola} \end{aligned} \tag{8}$$

The entire trajectory is created merging one after one straight lines and parabolas which are parametrized independently one from the other using a parameter range $u \in [0,1]$. This method simplifies the trajectory equation creation even though the evaluation of the motion profile of parameter u is get complicated as will be shown latter.

In fig.1 is possible to see the control points $\mathbf{p}_j$ defined in the workspace. They are used to interpolate the trajectory, linking straight lines with parabola trajectories in order to obtain a smooth path. The parabola trajectories are geometrically constructed defining points $\mathbf{p}_j^i$ and $\mathbf{p}_j^u$ which define input and output of the trajectory. They are obtained using construction lines intersected with circles with δ radius centred on vertices defined by $\mathbf{p}_j$. For a further generalization of the trajectory for the 3D space, and not only for the plane, suffices intersect the previous segments with spheres of δ radius centred in the vertices and correctly select the intersection points. To link straight lines using parabolas trajectories leads to final straight lines limited by points $\mathbf{p}_{j-1}^u$ and points $\mathbf{p}_j^i$ as it's easily understandable.

It's possible to evaluate derivatives of eq. 8 respect to variable u using formula 7.

Computing for straight and parabola lines $d\mathbf{b}/du$ and $d^2\mathbf{b}/du^2$ and exploiting equations 3, $\dot{u}(t)$ and $\ddot{u}(t)$ are obtained.

In this way all instruments needed to evaluate temporal derivatives of *Bézier curves* through the use of eq.3 are made available. Respectively for **straight**

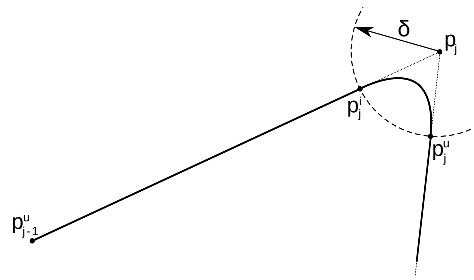

Figure 1: Control Points

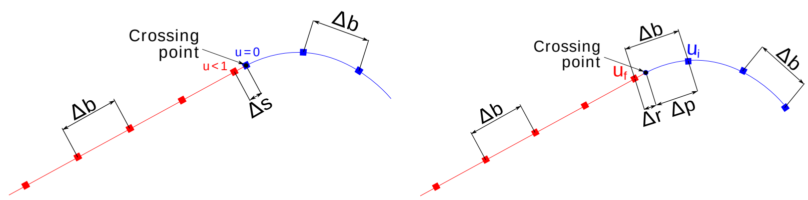

(a) Crossing point (b) Correction of the crossing point

Figure 2: Deposition trajectory

and **parabolic lines**:

$$\dot{\tilde{\mathbf{b}}}(t) = \left(-\mathbf{p}^u_{j-1} + \mathbf{p}^e_j\right)\dot{u} \qquad\qquad \ddot{\tilde{\mathbf{b}}}(t) = \left(-\mathbf{p}^u_{j-1} + \mathbf{p}^e_j\right)\ddot{u} \tag{9}$$

$$\begin{aligned}
\dot{\tilde{\mathbf{b}}}(t) &= -2\left(1-u\right)\dot{u}\mathbf{p}^e_j + \left[2\dot{u}\left(1-u\right) - 2u\dot{u}\right]\mathbf{p}_j + 2u\dot{u}\mathbf{p}^u_j \\
\ddot{\tilde{\mathbf{b}}}(t) &= \left[\dot{u}^2 - 2(1-u)\ddot{u}\right]\mathbf{p}^e_j + \left[2\ddot{u}(1-u) - 2\dot{u}^2 - 2u\ddot{u}\right]\mathbf{p}_j + \left(2\dot{u}^2 + 2u\ddot{u}\right)\mathbf{p}^u_j
\end{aligned} \tag{10}$$

Now it's possible to evaluate the motion profile computing the $u(t)$ values in every instant considering the time discretization with sample time T_s. The goal is to generate a TVP[1] for parameter $u(t)$ in order to guarantee a constant material flow in all trajectory points. For part with constant acceleration eq.5 is used whereas for the central part of the path eq.4 is used. Pulling together straight and parabolic segments a velocity variation of the parametric variable is

[1]trapezoidal velocity profile

generated in the first point of the new segment when passing from the previous to the following. That's caused by the fact that in the crossing point the parametric value is not $u = 1$ but it's lower as shown by fig.2a. Since every segment is defined by a starting parametric value $u = 0$ a spatial distance is generated along the path $\Delta s < \Delta b$ between the last point of the straight line and the initial point of the parabolic line. It's necessary to attribute a suitable value of u to the first point of the parabolic line in order to obtain equally spaced points along the path, equal to Δb. Having as reference fig.2b, and being aware that $\Delta b = v_c \cdot T_s$ and $\Delta r = b_{line}(u = 1) - b_{line}(u_f)$ it's necessary to evaluate the right variable u_2 to collocate the first point of the parabolic line to a distance equal to Δb along the curve evaluated as $\Delta p = \Delta b - \Delta r$.

Rewriting conveniently equation 4 for the parabolic line u_i is obtained as follow:

$$u_i = \frac{\Delta p}{\left|\frac{d\mathbf{b}}{du}\right|_{u=0}} - \frac{\Delta p^2}{2}\left[\frac{\frac{d\mathbf{b}^T}{du}\cdot\frac{d^2\mathbf{b}}{du^2}}{\left|\frac{d\mathbf{b}}{du}\right|^4}\right]_{u=0} \tag{11}$$

The same procedure with same rules is used for the crossing point from a parabolic to a straight line. It's possible to evaluate $\Delta r = \Delta b - \Delta p$ where $\Delta b = v_c \cdot T_s$ whereas for the evaluation of Δb is necessary to recall eq.4 replacing $u_{k+1} = 1$, $u_k = u_f$ and $v_c \cdot T_s = \Delta p$.

Replacing and rewriting an equation of second degree for the variable Δp is obtained:

$$\frac{1}{2}\left[\frac{\frac{d\mathbf{b}^T}{du}\cdot\frac{d^2\mathbf{b}}{du^2}}{\left|\frac{d\mathbf{b}}{du}\right|^4}\right]_{u_f}\Delta p^2 - \frac{1}{\left|\frac{d\mathbf{b}}{du}\right|_{u_f}}\Delta p + 1 - u_f = 0 \tag{12}$$

Solving with respect to Δp is computed u_i on the straight line replacing it

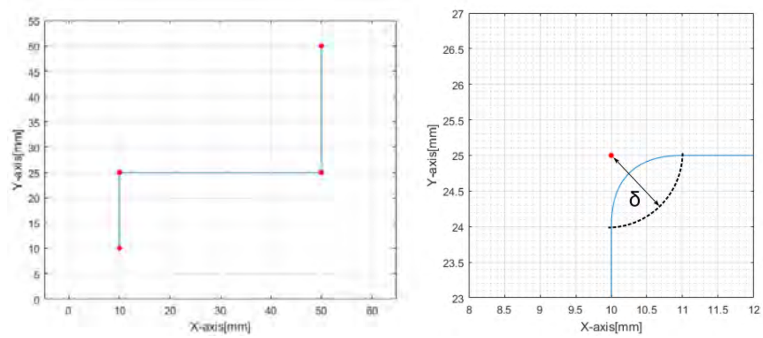

(a) trajectory example (b) error δ

Figure 3: Trajectory generated with a Bézier curve algorithm

in the equation 4:

$$u_i = \frac{\Delta r}{\left|\dfrac{d\mathbf{b}}{du}\right|_{u=0}} \tag{13}$$

4.1. Example

In this section we show a theoretical example of the use of Bézier curves. The process is carried out starting from a set of N points. The parameter inputs of this algorithm are the velocity to reach, $\dot{u}$ which is kept constant along the central part of the trajectory, and δ, which defines the maximum distance of one point from the trajectory generated, and so can be considered as the maximum error in a production process. Starting from a first point with a null velocity the algorithm takes into account three points at the time, fig.1, generating the trajectory until the final point is reached with a null velocity.

In fig.3 is shown a trajectory generated considering four points highlighted in red. If we look closely it's possible to see how the middle points of the trajectory are not touched by the trajectory itself but the maximum distance of any point from the trajectory is lower than δ. In this way δ can be considered as measure of the process accuracy.

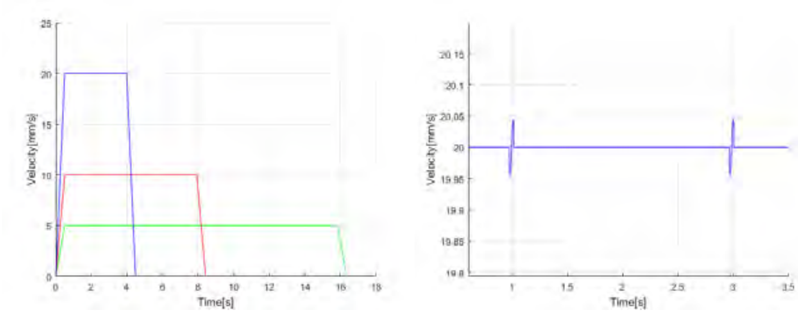

(a) Deposition velocity (b) Velocity oscillation

Figure 4: Parametric velocity $\dot{u}$

$\dot{u}_c$[mm/s]	Percentage variation
5	0.14
10	0.27
20	0.22

Three different parametric velocity $\dot{u}$ have been set as 5, 10 and 20[mm/s], fig.4a. All the velocities have a trapezoidal velocity profile where the maximum velocity reached is equal to the constant velocity, $\dot{u}_c$, that we want to maintain along all the central part of the path. During the central part of the trajectory the velocity can be considered constant with minor oscillations. If we look closely, fig.4b, it's possible to see how during the two curves of the path there is a little variation in the parametric velocity $\dot{u}$. For the three velocities tried the percentage variation in the velocity with respect to $\dot{u}_c$ is always smaller than 0.3%,

5. Path Planning using Rational Bézier Curves

The path planning approach described in Section 4 can be further extended to improve the interpolation of the ideal trajectory, at the cost of a higher complexity of the calculations. This could be rather relevant in the cases where

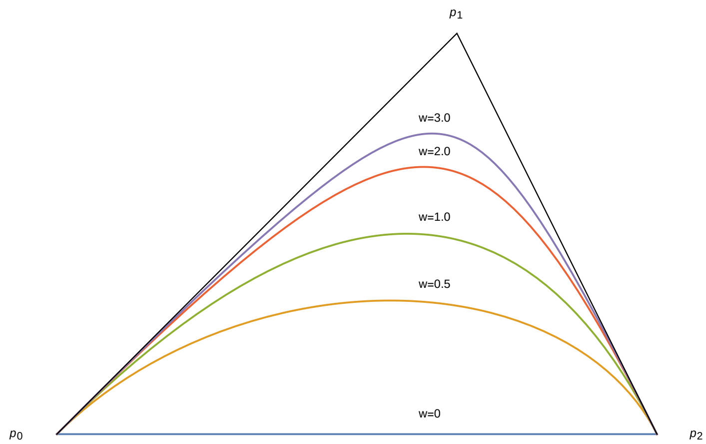

Figure 5: Rational Bézier Curves with different w.

a higher accuracy is required and where different kinds of accuracies are required in different points of the trajectory. A different interpolation approach is adopted, using a *Rational Bézier Curve*, i.e., a curve in $\mathbb{R}$ with $d = 2, 3$, being the projection of a polynomial Bézier curve in $\mathbb{R}^{d+1}$.

Given a set of control points $\mathbf{p}_j \in \mathbb{R}$ and a set of weights $w_j \in \mathbb{R}$ with $w_j \geq 0$, a *Rational Bézier Curves*, defined over the interval $[0, 1]$, can be written as:

$$\mathbf{R}(u) = \frac{\sum_{j=0}^{m} B_j^m(u) \cdot w_j \cdot \mathbf{p}_j}{\sum_{j=0}^{m} B_j^m(u) \cdot w_j} \tag{14}$$

If $w_j = 1 \forall j$, the rational Bézier curve is equal to a polynomial Bézier curve. Increasing the weight w_j pulls the curve to the control point $[p]_j$ while decreasing the weight $w - j$ pushes the curve away from it (Figure 5). In the limit case, when $w_j \to \infty$, the interpolation curve tends to the piecewise linear sequence of segments joining the points.

In a similar way, the results related to the differentiation of Rational Bézier Curves could be exploited [20]. The derivative of a rational bézier curve in its general form is:

$$\mathbf{P}^{'}(u) = \sum_{j=0}^{m-1} \lambda_j(u)(\mathbf{P}_{j+1} - \mathbf{P}_i) \tag{15}$$

where, for $j = 0, \ldots, m-1$,

$$\lambda_j(u) = \frac{1}{(1-u)uw_{0,m}^2(u)} \sum_{i=0}^{j} \sum_{k=j+1}^{m} (k-i)B_{j,m}(u)B_{k,m}(u)w_i w_k \tag{16}$$

where $B_{i,m}(u)$ are the Bernstein polynomials and the weights $w_{i,k}(u)$ are defined as:

$$\sum_{j=0}^{k} B_{j,k}(u)w_{i+j} \tag{17}$$

Let us consider a quadratic curve defined by three points:

$$\mathbf{P}(u) = \frac{(1-u)^2\mathbf{p}_1 + 2wu(1-u)\mathbf{p}_2 + u^2\mathbf{p}_3}{(1-u)^2 + 2wu(1-u) + u^2} \tag{18}$$

$$\begin{aligned}
\lambda_0(u) &= \frac{1}{(1-u)uw_{0,2}^2(u)} \sum_{j=0}^{0} \sum_{k=1}^{2} kB_{j,2}(u)B_{k,2}(u)w_j w_k = \\
&= \frac{1}{(1-u)uw_{0,2}^2(u)} [1B_{0,2}(u)B_{1,2}(u)w_0 w_1 + 2B_{0,2}(u)B_{2,2}(u)w_0 w_2] = \\
&= \frac{1}{(1-u)uw_{0,2}^2(u)} [(1-u)^2 2u(1-u)w_0 w_1 + 2(1-u)^2 u^2 w_0 w_2]
\end{aligned} \tag{19}$$

$$\begin{aligned}
\lambda_1(u) &= \frac{1}{(1-u)uw_{0,2}^2(u)} \sum_{j=0}^{1} \sum_{k=2}^{2} (k-j)B_{j,2}(u)B_{k,2}(u)w_j w_k = \\
&= \frac{1}{(1-u)uw_{0,2}^2(u)} [(2-0)B_{0,2}(u)B_{2,2}(u)w_0 w_2 + (2-1)B_{1,2}(u)B_{2,2}(u)w_1 w_2] = \\
&= \frac{1}{(1-u)uw_{0,2}^2(u)} [2(1-u)^2 u^2 w_0 w_2 + 2u(1-u)u^2 w_0 w_2]
\end{aligned} \tag{20}$$

where,

$$\begin{aligned}
w_{0,2}(u) &= \sum_{j=0}^{2} B_{j,2}(u)w_j = B_{0,2}(u)w_0 + B_{1,2}(u)w_1, B_{2,2}(u)w_2 = \\
&= (1-u)^2 w_0 + 2u(1-u)w_1 + u^2 w_2
\end{aligned} \tag{21}$$

To obtain the first derivative of the rational Bézier curve, the expressions of $\lambda_0(u)$ and $\lambda_1(u)$ must be substituted in:

$$\mathbf{P}^{'}(u) = \lambda_0(u)(\mathbf{p}_1 - \mathbf{p}_0) + \lambda_1(u)(\mathbf{p}_2 - \mathbf{p}_1) \tag{22}$$

The expression of the second derivative is more complex [20]:

$$\begin{aligned}\mathbf{P}^{''}(u) = {} & m\frac{w_{2,m-2}(u)}{w_{0,m}^3(u)}(2mw_{0,m-1}^2 - (m-1)w_{0,m-2}w_{0,m} - 2w_{0,m-1}w_{0,m})(P_{2,m-2}(u) - P_{1,m-2}(u)) \\ & - m\frac{w_{0,m-2}(u)}{w_{0,m}^3(u)}(2mw_{1,m-1}^2(u) - (m-1)w_{2,m-1}w_{0,m} - 2w_{1,m-1}w_{0,m})(P_{1,m-2}(u) - P_{0,m-2}(u))\end{aligned} \tag{23}$$

where

$$\mathbf{P}_{i,k}(u) = \frac{\sum_{j=0}^{k} B_{j,k}(u)w_{i+j}\mathbf{p}_{i+j}}{\sum_{j=0}^{k} B_{j,k}(u)w_{i+j}} \tag{24}$$

The approach described in Section 4 can be applied using these expression for the calculation of $\dot{u}(t)$ and $\ddot{u}(t)$ to calculate the values of $u(t)$ according to the discretization adopted. The use of different weights can allow different degrees of accuracy along the trajectory.

6. Application to an additive manufacturing machine prototype

The path algorithm described has been applied in an innovative additive manufacturing technique designed at the Politecnico di Milano[5]. This technique is based on a metal injection molding (MIM) extruder shown in Fig.6. A feedstock of metal powder and polymeric binder is poured in the right side of the machine where is heated and pressed in a downstream chamber from wherein it is extruded. The so called *green body* obtained is then sintered to obtain the final object. This technique is candidated to be an alternative AM techniques for metal printing, where usually laser or electron based melting techiques are used, whose costs is rather high. In Fig.6 it also possible to see the two electrical

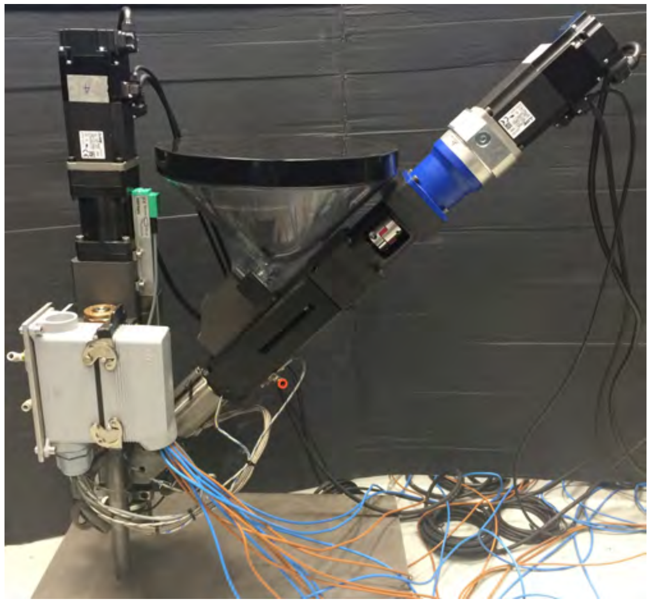

Figure 6: Extrusion system

motors controlling the extrusion system. One motor pushes the feedstock in the final chamber where the material is extruded through a piston controlled by the other motor. Controlling the extrusion motor is the main drive to control the process and, hence, obtain a constant extrusion rate. The extrusion system is mounted on a machine structure described in the following part of the paragraph. The machine architecture is based on a linear delta robot, where a mobile platform is moved to implement the path obtained through the described path planning algorithm. The parametric velocity associated to the movement of the platform is calibrated together with the extrusion rate of the devices in Fig.6.

Differently from traditional cartesian CNC machines, the G-code must be further processed, to obtain a trajectory in terms of $\mathbf{p}_j$ points to be processed by the path generation algorithm. Once the path in the space is obtained, the inverse kinematic equations associated to the machine architecture are used to derive the trajectories for the actuators. in the current version of the machine prototype, these steps are operated off-line. A motion control CPU together

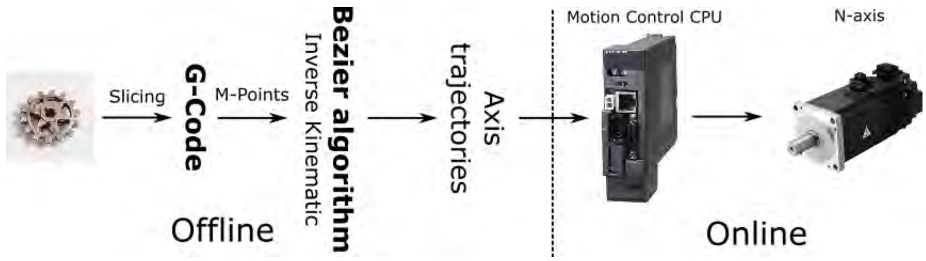

Figure 7: Path algorithm implementation

with servo systems closes the control loops for each actuator.

6.1. Machine Design

In Fig.8. the previously described machine prototype is shown, designed by the authors in [4]. The picture on the left shows the delta robot architecture capable to translate the platform where the extruded material is laid down. The picture on the right shows the control system based on PLCs and a module for the motion control of the three motion axis and the two motors of the extruder. The linear delta moves the platform in accordance with the extrusion rate of the extruder which is going to be installed on the top of the machine (Fig.9a). The three axis managed by the motion control module correspond to the displacement of three sliders along the three linear guides visible in Fig.8a. The motion module also controls the extruder through its two motors and keep velocity of the motor driving the extrusion rate constant to guarantee a constand material deposition in time, jointly controlling the parametric velocity of the platform following the desired trajectory.

6.2. Testing

The actual implementation of a trajectory in an industrial machine pass through the possibility of the machine actuators to actually execute the trajectory generated. In order to demonstrate the feasibility of this approach a practical test has been executed on the AM machine aforementioned. The trajectory defined through the proposed algorithm has been first tested in a

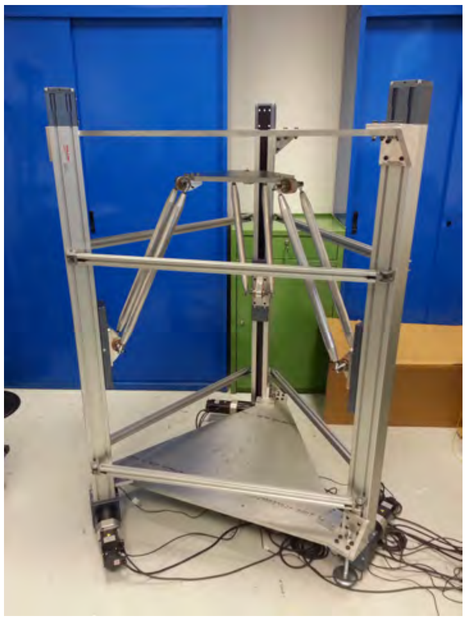

(a) Linear Delta

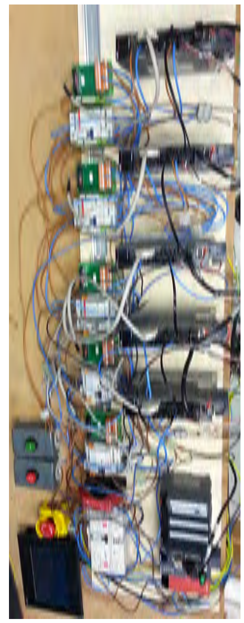

(b) Control System

Figure 8

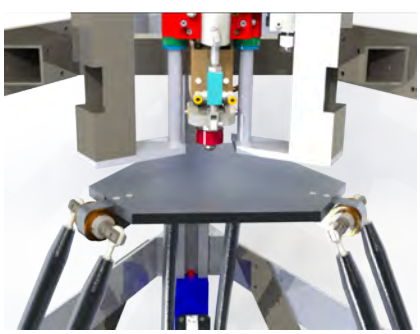

(a) AM machine

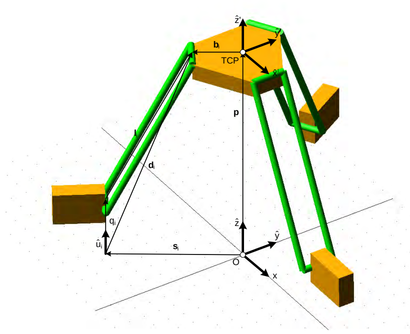

(b) Dynamic Model

Figure 9

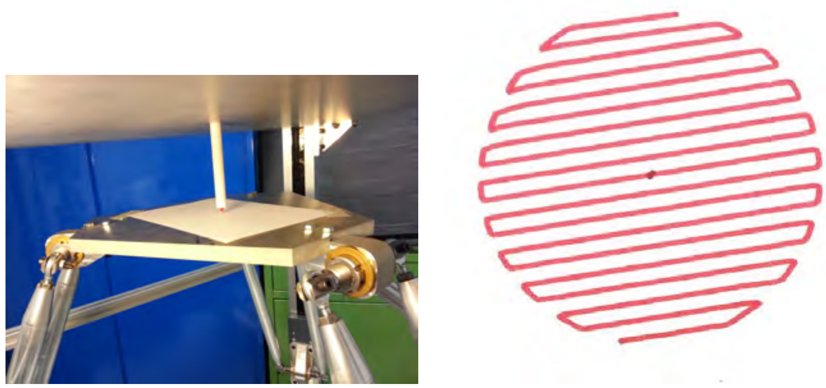

(a) Deposition System

(b) Drawing

Figure 10: Deposition application

dynamic model of the system created using the Adams®software9b. This environment provide the capability of estimating the torques and accelerations of the motors, given a path to be executed. The analysis of the results clearly show that a constant parametric velocity in the trajectory (and, hence, of the platform) causes acceleration peaks of the motors. Moreover, small fluctuations of the platform velocity cannot be avoided. Nevertheless, for this AM application, the magnitude of these fluctuations is negligible.

After the simulation, the proposed path algorithm has been used to derive an exemplary path to be tested on the machine prototype.

To decouple the performance of the path planning approach from the characteristics of the extruder, a red pen has been used as end effector to draw the movements of the platform on a paper sheet (Fig.10a). The path obtained is shown in Fig.10b.

To see the feasibility of the process it is worth to compare the parametric velocity $\dot{u}$ of the platform and the accelerations obtained on the active joints of the machine. In Fig.11b, the blue circle represents the desired path for the platform. It has been evaluated starting from $\mathbf{p}_j$ points obtained intersecting a circle with straight lines and, hence, simulating the results of a slicing procedure.

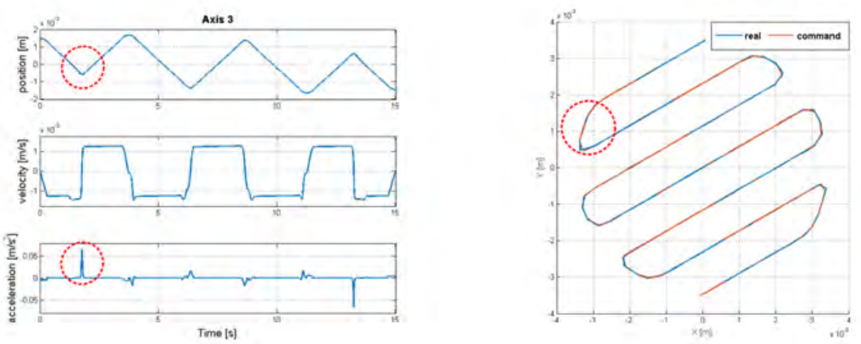

(a) axis 3

(b) Platform trajectory

Figure 11

Hence, the interpolation has been used to evaluate the platform trajectory. The red circle, matching almost perfectly the blue one, is the real platform trajectory, evaluated measuring the position of the motors through their encoders and using the direct kinematics equations. The implementation of the system on an industrial architecture leads to small position errors during the movements. The parametric velocity $\dot{u}$ has been set to $5[mm/s]$ and a fillet radius $\delta = 0.45[mm]$ has been chosen. No weight has been used in this example by not having points more important than others along the trajectory. Looking at Fig.11a, it is interesting to notice how, even with a constant parametric velocity, acceleration peaks affects the motors, whose entity could possibly be infeasible. Actually, constant parametric velocity along the deposition path leads to high accelerations in the curves. Looking the details, it can be seen how acceleration peaks appear in correspondence with the inversion of the direction of axis 3, which corresponds to the curves of the path reported in Fig.11b.

The change of direction of the axis, its corresponding acceleration peak and the trajectory curve of the platform are highlighted with red circles. The acceleration peaks lead to small velocity fluctuations along the path of the linear delta platform as expected.

7. Conclusions

Depending on the technology being used, there are different suitable path-planning methodologies one can use in order to achieve a specific goal. The focus of this paper is to propose an original approach based on the Bezier curves, useful in the cases where a constant velocity along the trajectory is required, for example, to facilitate a deposition of material obtained by extrusion.

This approach is presented, developed and tested here for an innovative additive manufacturing process but it is suitable also for other industrial field such as painting, gluing and aerosol spraying. The algorithm is capable of ensuring a constant velocity along the path of the TCP with very slight oscillations.

In order to clarify this approach the mathematical treatment is presented and a test case described. In particular it has been applied to a prototype of 3d printer based on a parallel kinematic and controlled by an industrial PLC and a motion control unit. This test case is particularly significant because due to the kinematic architecture the control of the velocity of the working table can generates high acceleration and high velocity on the actuators. A mechanical model of the system has been developed in order to analyse the torque and acceleration required to the actuators and verify the applicability of the path-planning approach proposed.

The results achieved are good and the method has been used to develop the technology on the basis of a new 3D printing solution for metal parts based on an MIM technique.

Bibliography

[1] I. Stratasys, modeling apparatus for three-dimensional objects, US Patent 5340433.

[2] D.Roberson, C.M.Shemelya, E.MacDonald, R.Wicker, Expanding the applicability of fdm-type technologies through materials development, Rapid Prototyping Journal 21 (2015) 137 – 143.

[3] N.Volpato, D.Kretschek, J.A.Foggiatto, C. da Silva Cruz, Experimental analysis of an extrusion system for additive manufacturing based on polymer pellets, International Journal of Advanced Manufacturing Technology 81 (2015) 1519–1531.

[4] E.Fiore, H.Giberti, L.Sbaglia, Dimensional synthesis of a 5-dof parallel kinematic manipulator for a 3d printer, in: 16th International Conference on Research and Education in Mechatronics REM, 2015.

[5] H.Giberti, M. Strano, M. Annoni, An innovative machine for fused deposition modeling of metals and advanced ceramics, in: MATEC Web of Conferences, 2016.

[6] H.Giberti, E.Fiore, L.Sbaglia, Kinematic synthesis of a new 3d printing solution, in: MATEC Web of Conferences, 2016.

[7] O.A.Mohamed, S.H.Masood, J.L.Bhowmik, Optimization of fused deposition modeling process parameters for dimensional accuracy using i-optimality criterion, Measurement 81 (2016) 174–196.

[8] A.Boschetto, V.Giordano, F.Veniali, Modelling micro geometrical profiles in fused deposition process, International Journal of Advanced Manufacturing Technology 61 (2012) 945–956.

[9] Y.Jin, J.Zhang, Y.Wang, Z.Zhu, Filament geometrical model and nozzle trajectory analysis in the fused deposition modeling process, Journal of Zhejiang University SCIENCE A.

[10] K. Jiang, Y. Gu, Controlling parameters for polymer melting and extrusion in fdm, Key Engineering Materials.

[11] P. Kulkarni, D. Dutta, Deposition strategies and resulting part stiffnesses in fused deposition modeling, Journal of Manufacturing Science and Engineering.

[12] G. Jin, W. Li, C. Tsai, L. Wang, Adaptive tool-path generation of rapid prototyping for complex product models, Journal of Manufacturing Systems.

[13] G. Jin, W. Li, L.Gao, An adaptive process planning approach of rapid prototyping and manufacturing, Robotics and Computer-IntegratedManufacturing.

[14] J. Mireles, D. Espalin, D. Roberson, B. Zinniel, F. Medina, R. Wicker, Fused deposition modeling of metals, 23rd Annual International Solid Freeform Fabrication Symposium - An Additive Manufacturing Conference.

[15] O. RISHI, Feed rate effects in freeform filament extrusion (2012/2013).

[16] B.Thompson, H.S.Yoon, Efficient path planning algorithm for additive manufacturing systems, IEEE Transactions on Components, Packaging and Manufacturing Technology 4 (2014) 1555–1563.

[17] Y.A.Jin, Y.He, J. W. Z. Lin, Optimization of tool-path generation for material extrusion-based additive manufacturing technology, Additive Manufacturing 1 (2014) 32–47.

[18] B.Sencer, K.Ishizaki, E.Shamoto, A curvature optimal sharp corner smoothing algorithm for high-speed feed motion generation of nc systems along linear tool paths, Int.J. of Advanced Manufacturing Technology 76 (2015) 1977–1992.

[19] L. Biagiotti, C. Melchiorri, Trajectory planning for automatic machines and robots, Springer Berlin Heidelberg.

[20] S. Floater, Derivatives of rational bézier curves, Computer Aided Geometric Design 9 (1992) 161–174.

axis3.png

Click here to download high resolution image

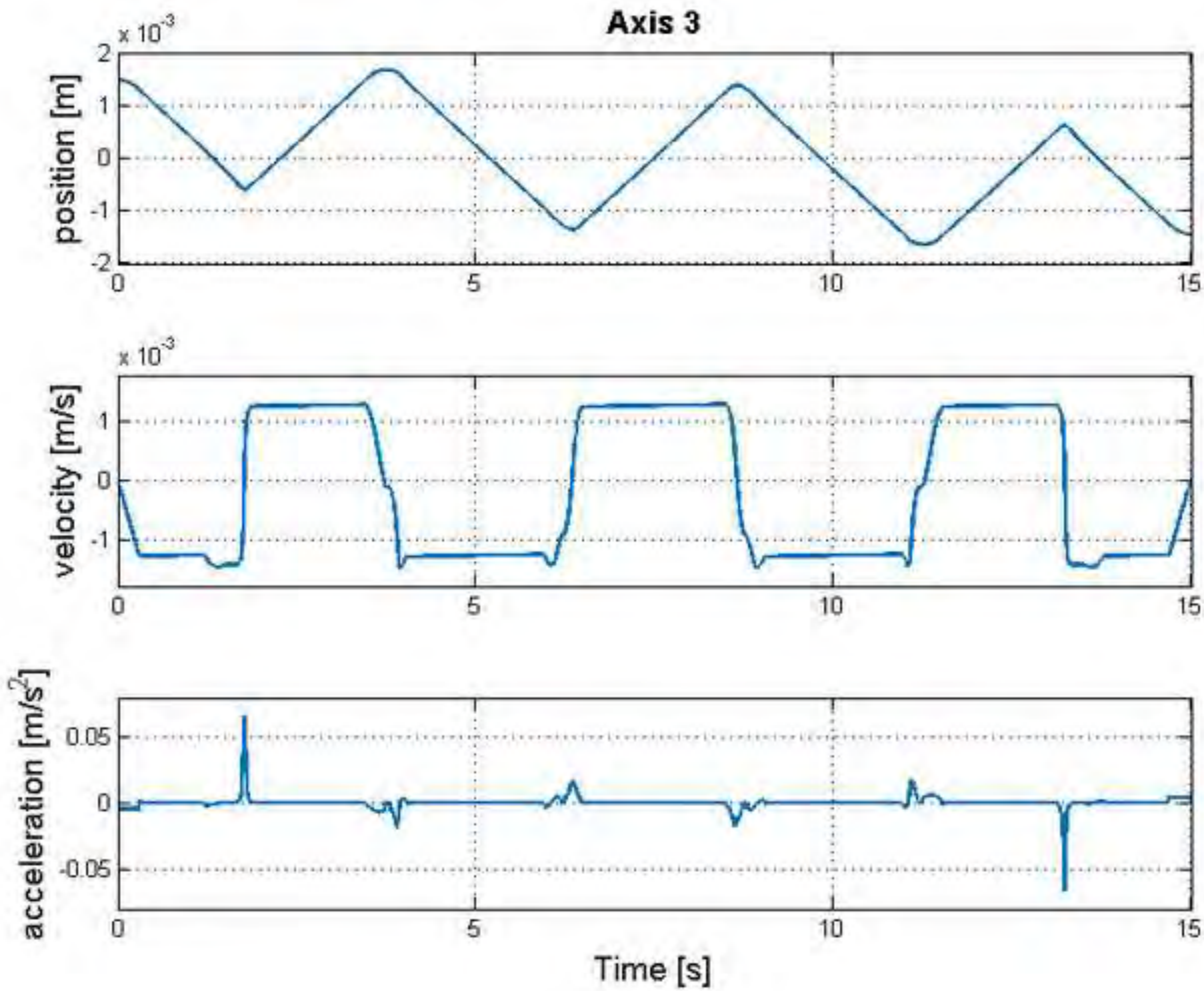

axis3_2.png
Click here to download high resolution image

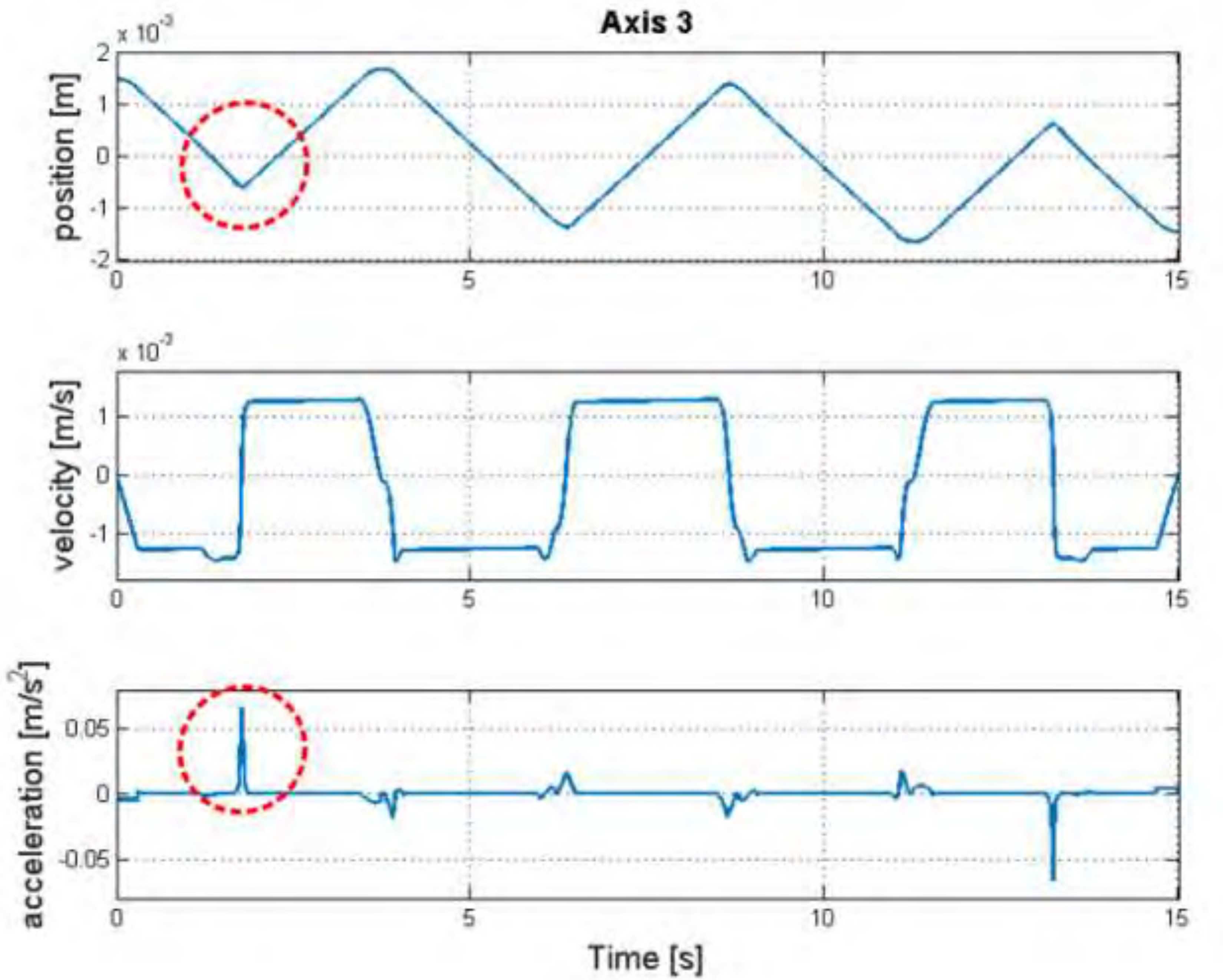

circle.png

Click here to download high resolution image

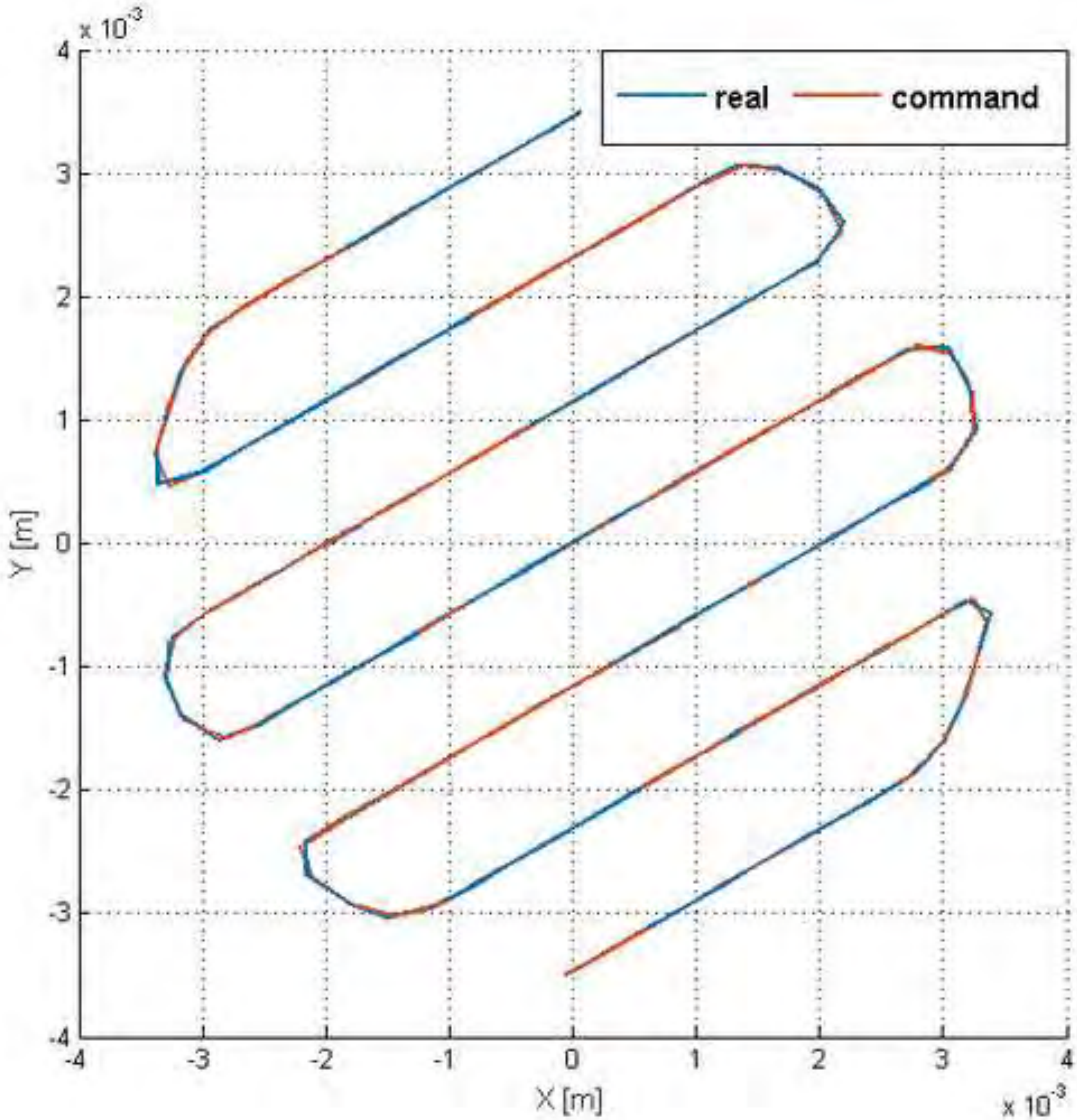

circle_2.png
Click here to download high resolution image

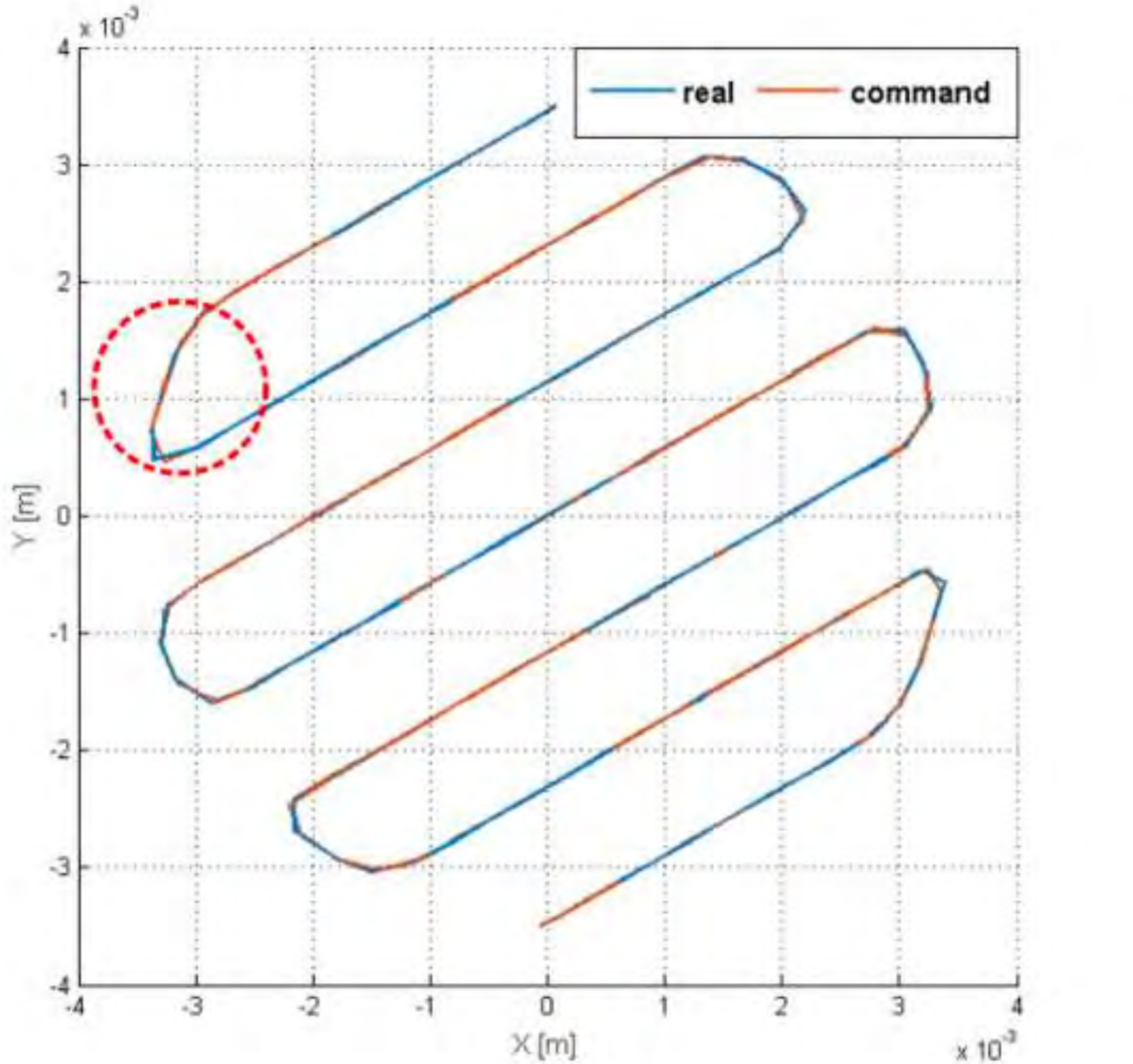

controllo.jpg

Click here to download high resolution image

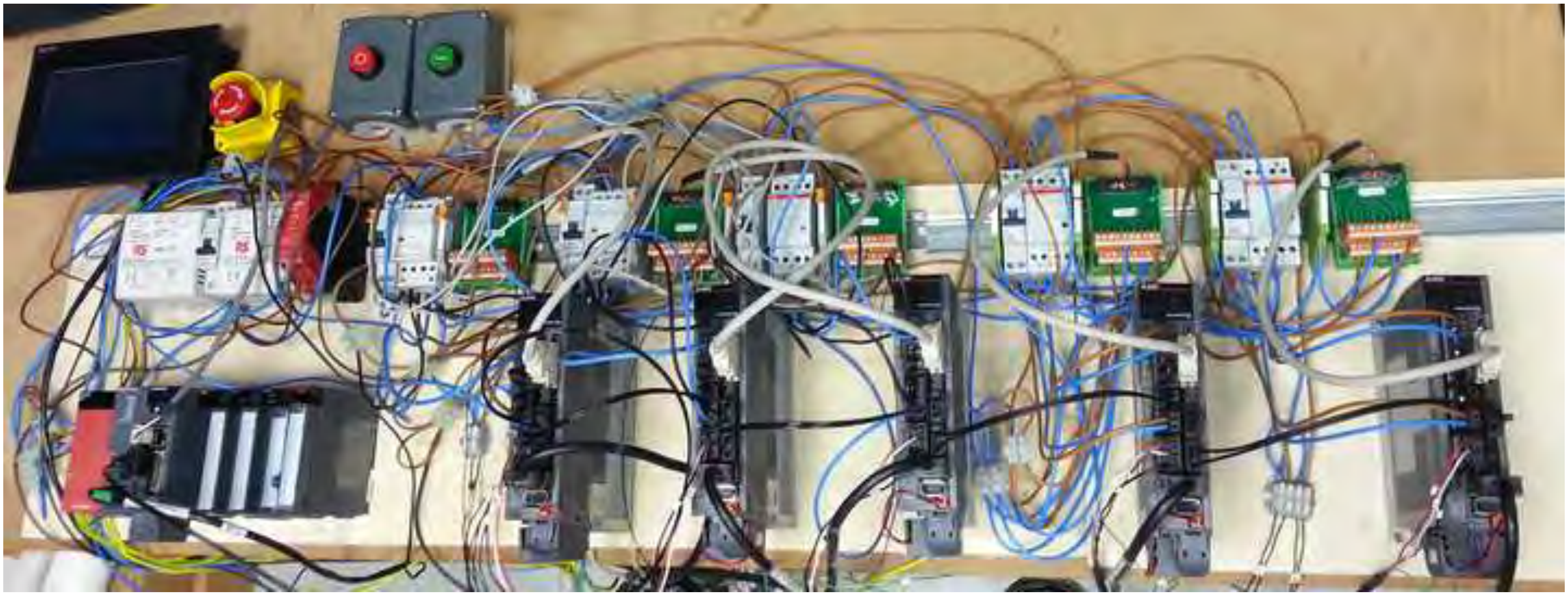

delta.pdf

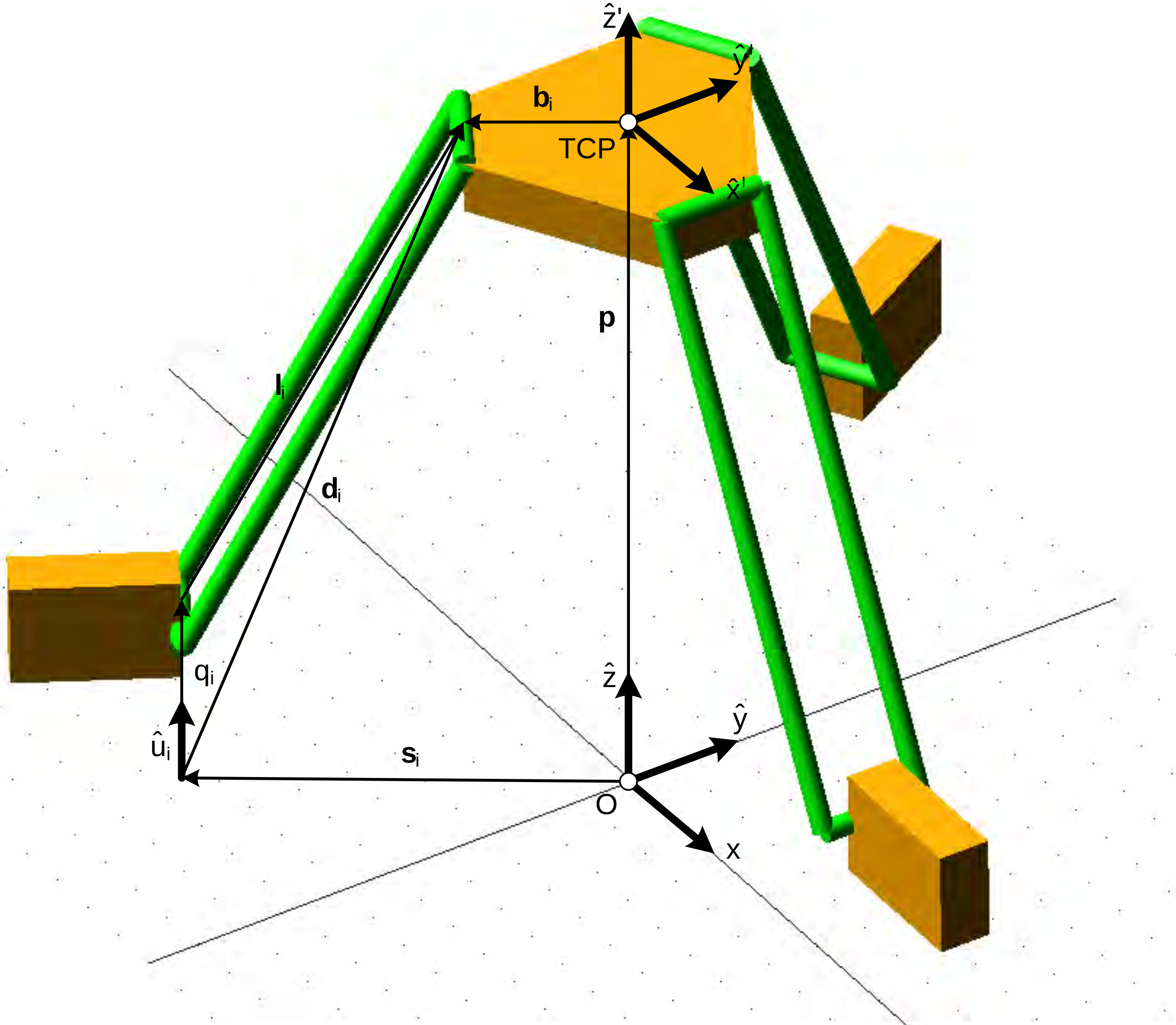
ẑ'
ŷ'
$\mathbf{b}_i$
TCP
x̂'
p
$\mathbf{l}_i$
$\mathbf{d}_i$
ẑ
ŷ
q_i
$\hat{u}_i$
$\mathbf{s}_i$
O
x

drawing.jpg
Click here to download high resolution image

estrusore.png

Click here to download high resolution image

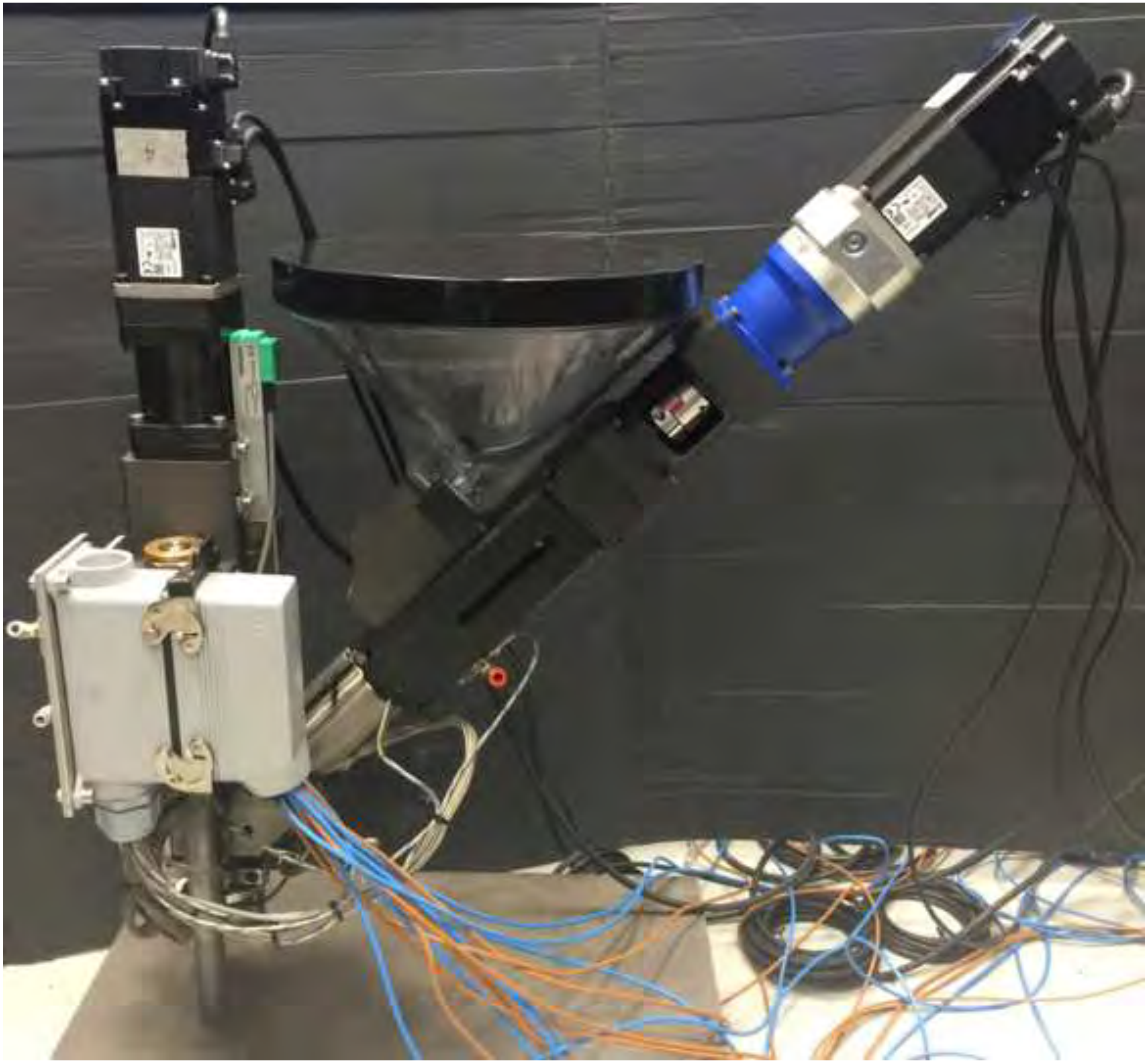

example1.png
Click here to download high resolution image

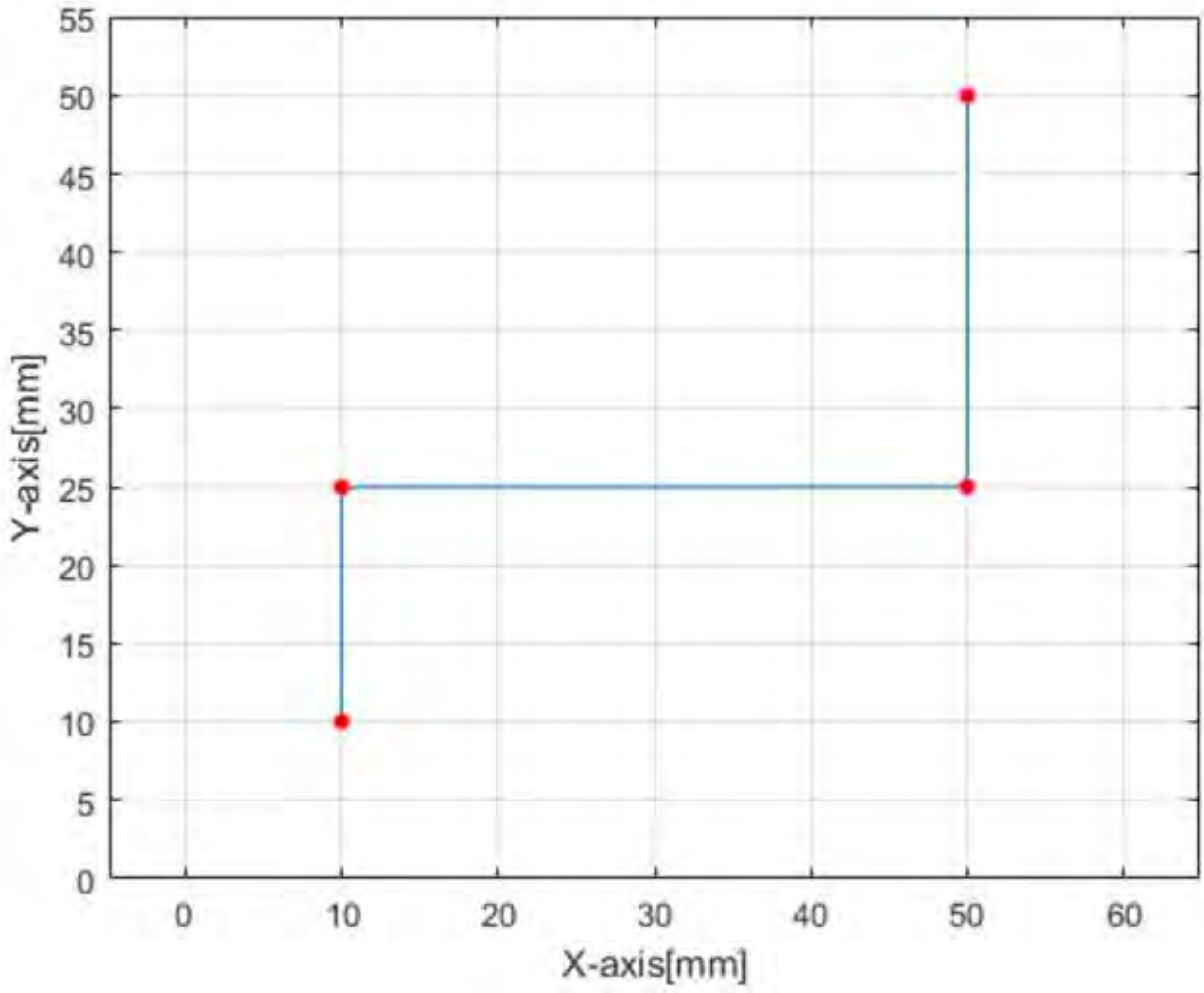

example2.png

Click here to download high resolution image

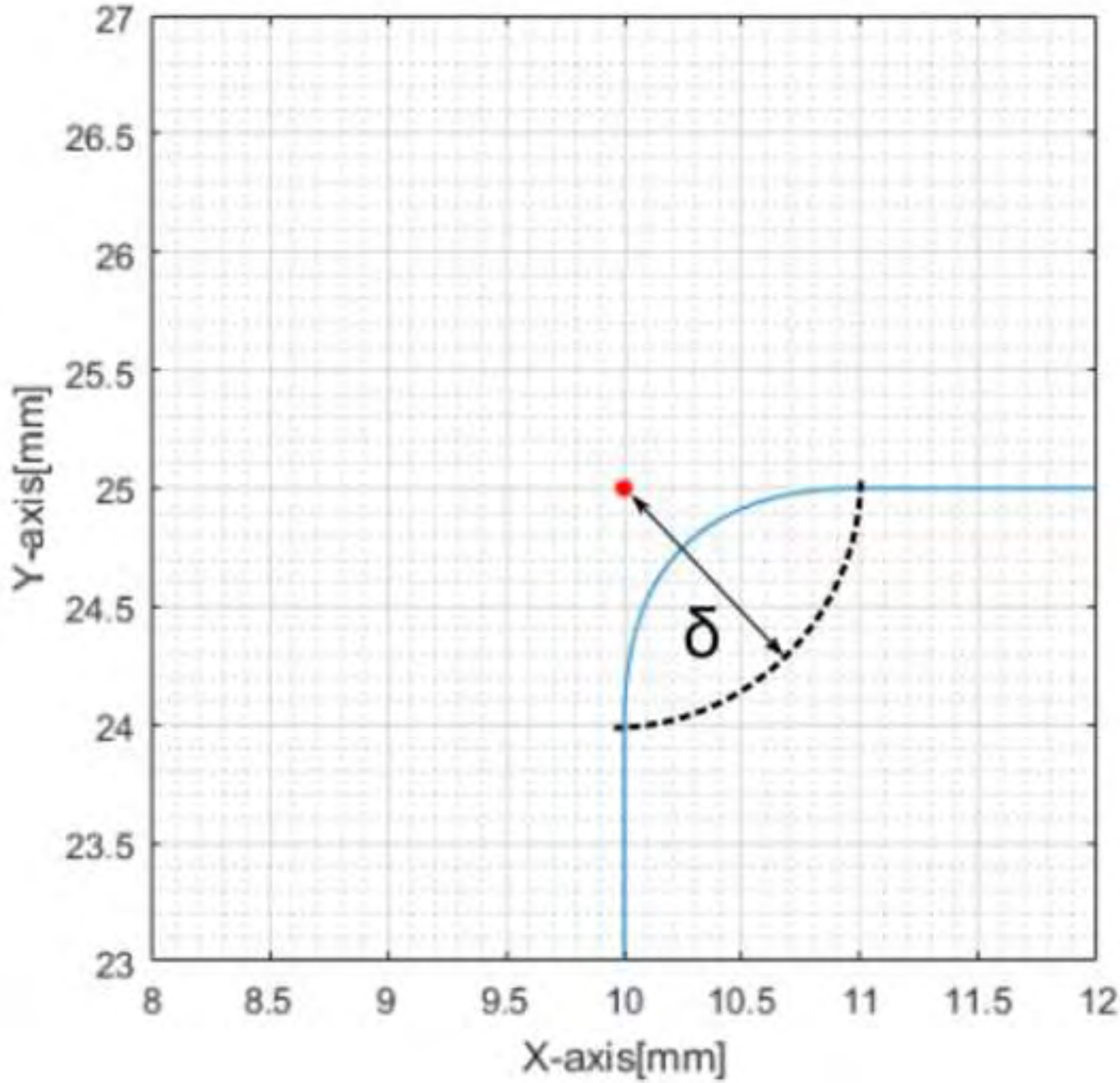

linear.jpg
Click here to download high resolution image

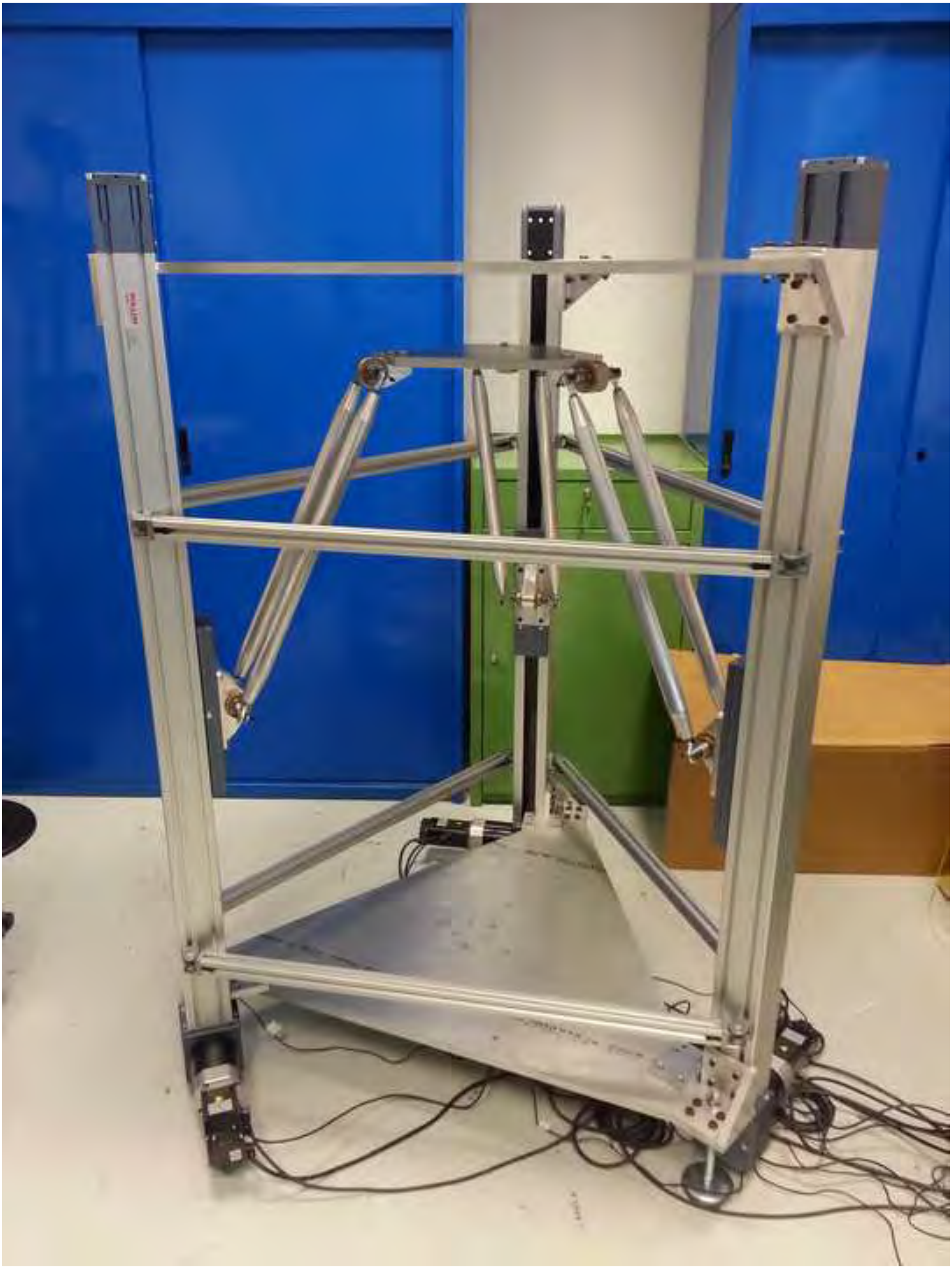

motion_routine.png

Click here to download high resolution image

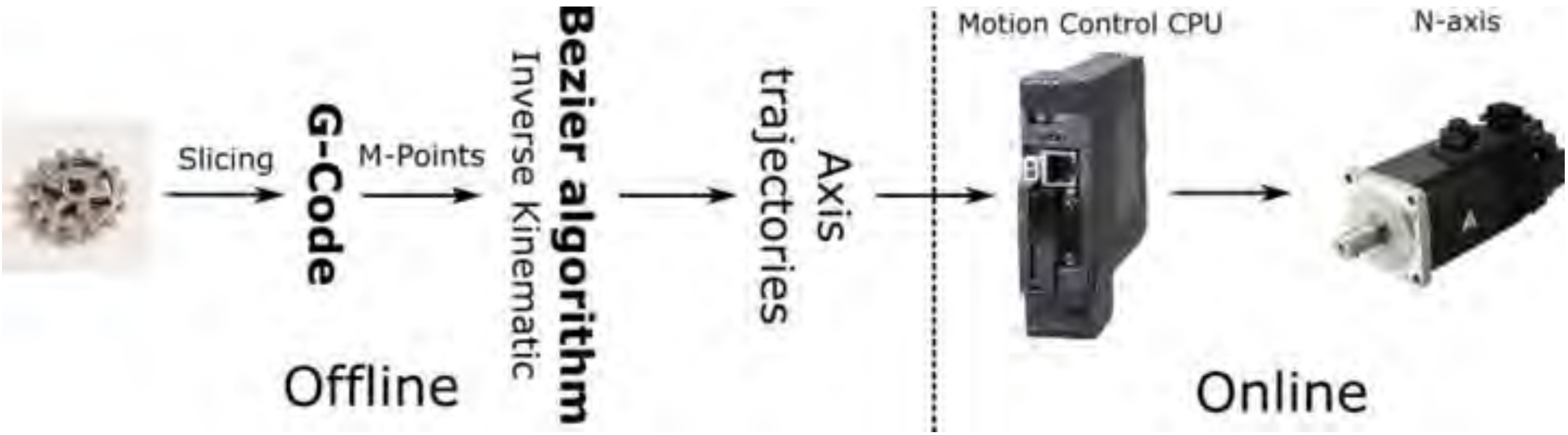

pennarello.jpg

Click here to download high resolution image

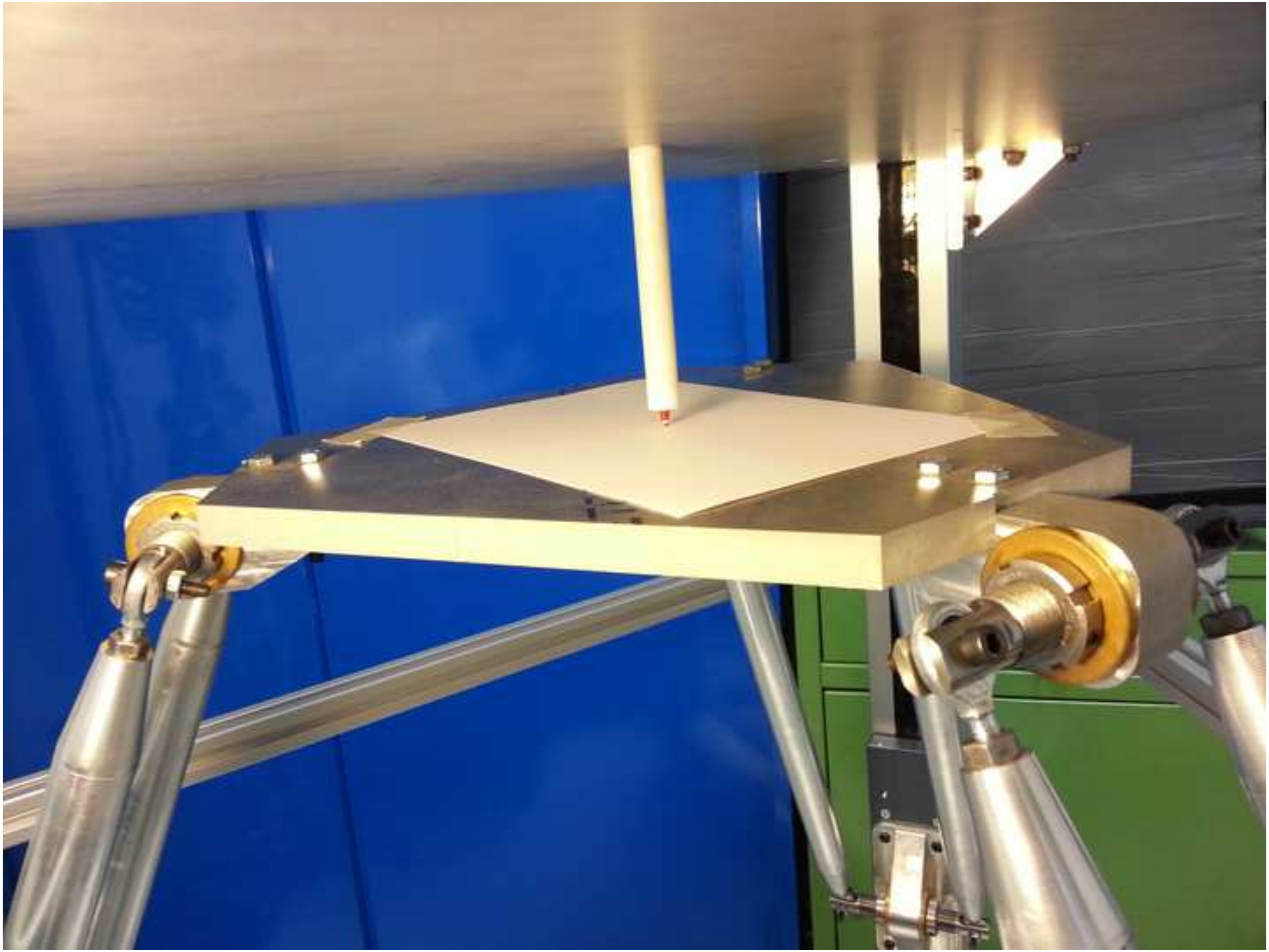

rationalbezierexample.pdf

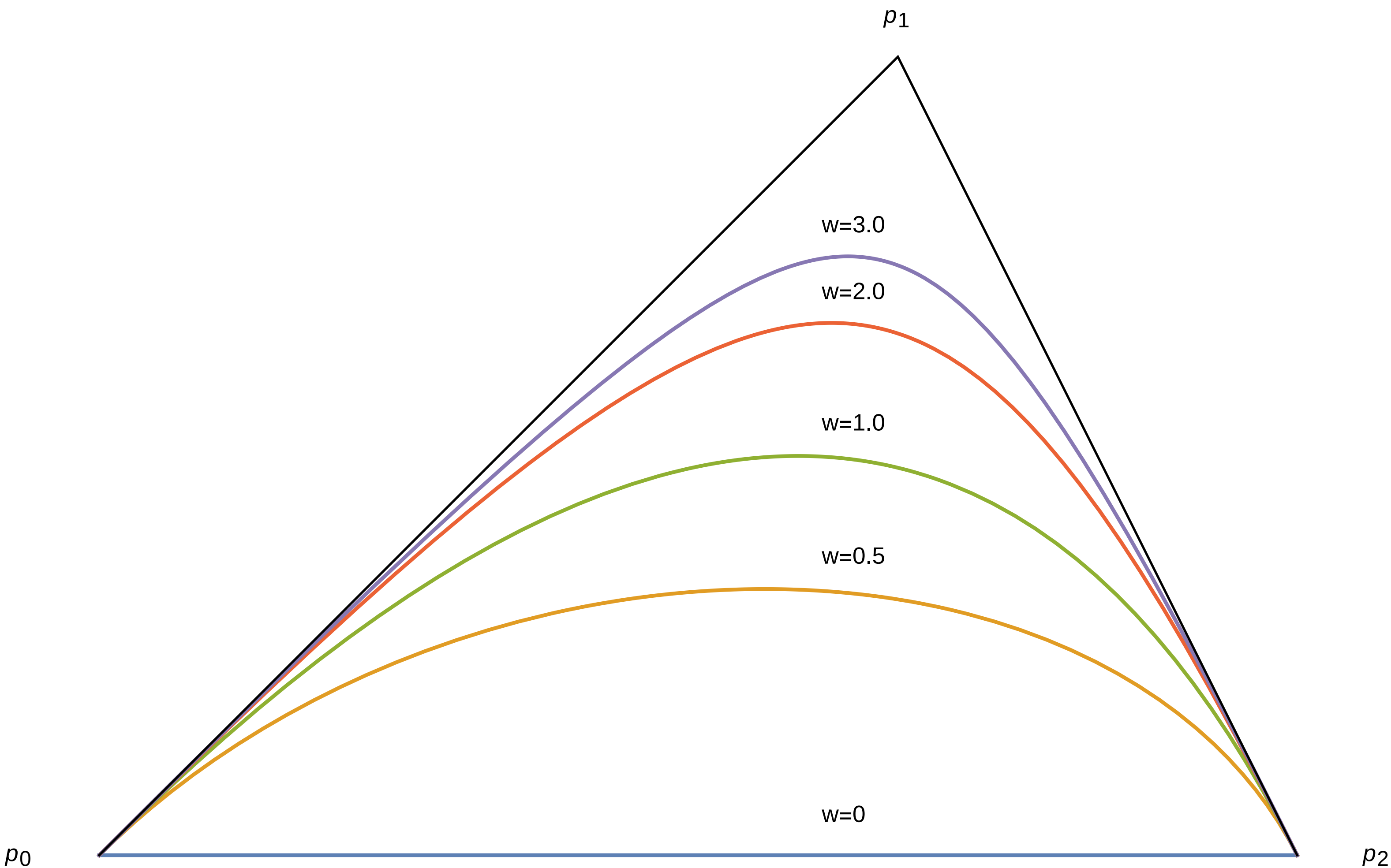

rendering.png
Click here to download high resolution image

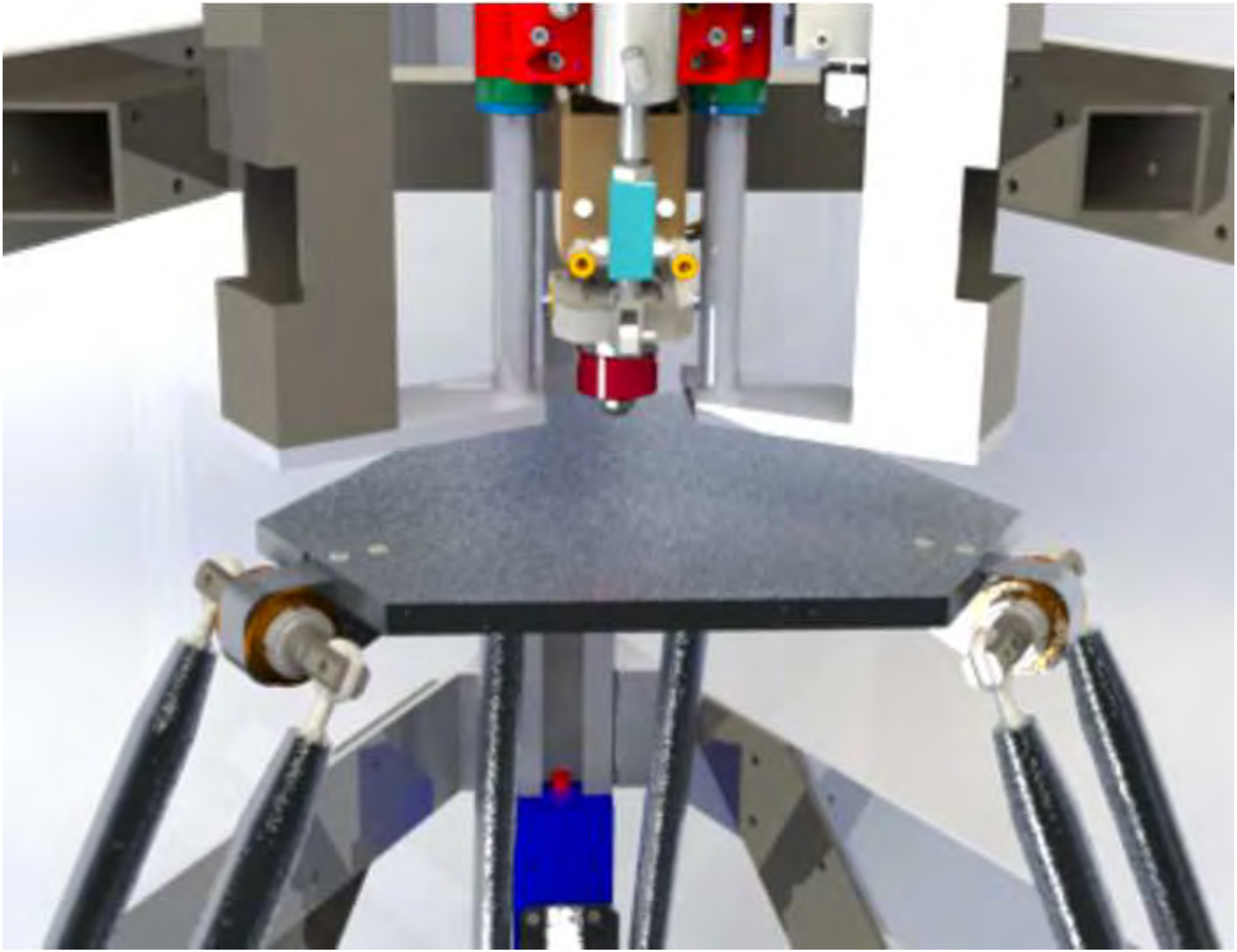

rendering2.png

Click here to download high resolution image

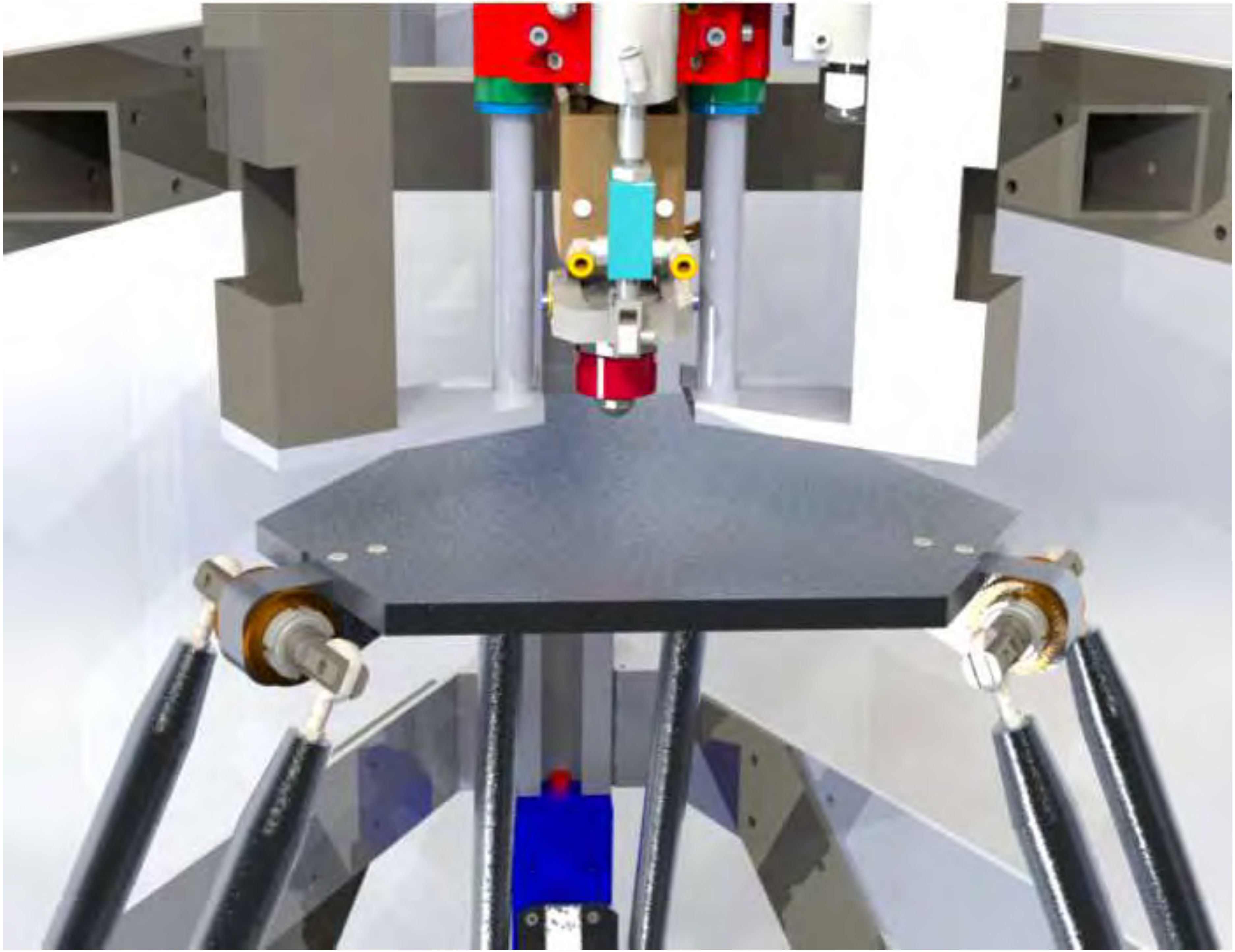

rette-para.pdf

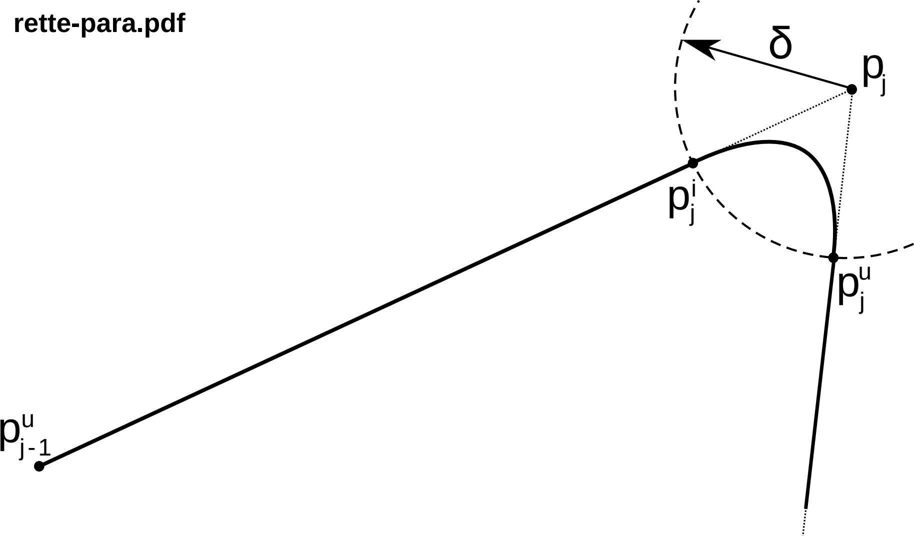

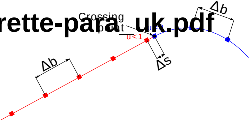

Δb
Crossing
point
u<1
Δs
Δb

rette-para_uk_corrett

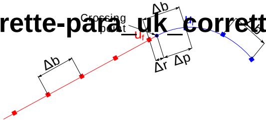

velocity.png
Click here to download high resolution image

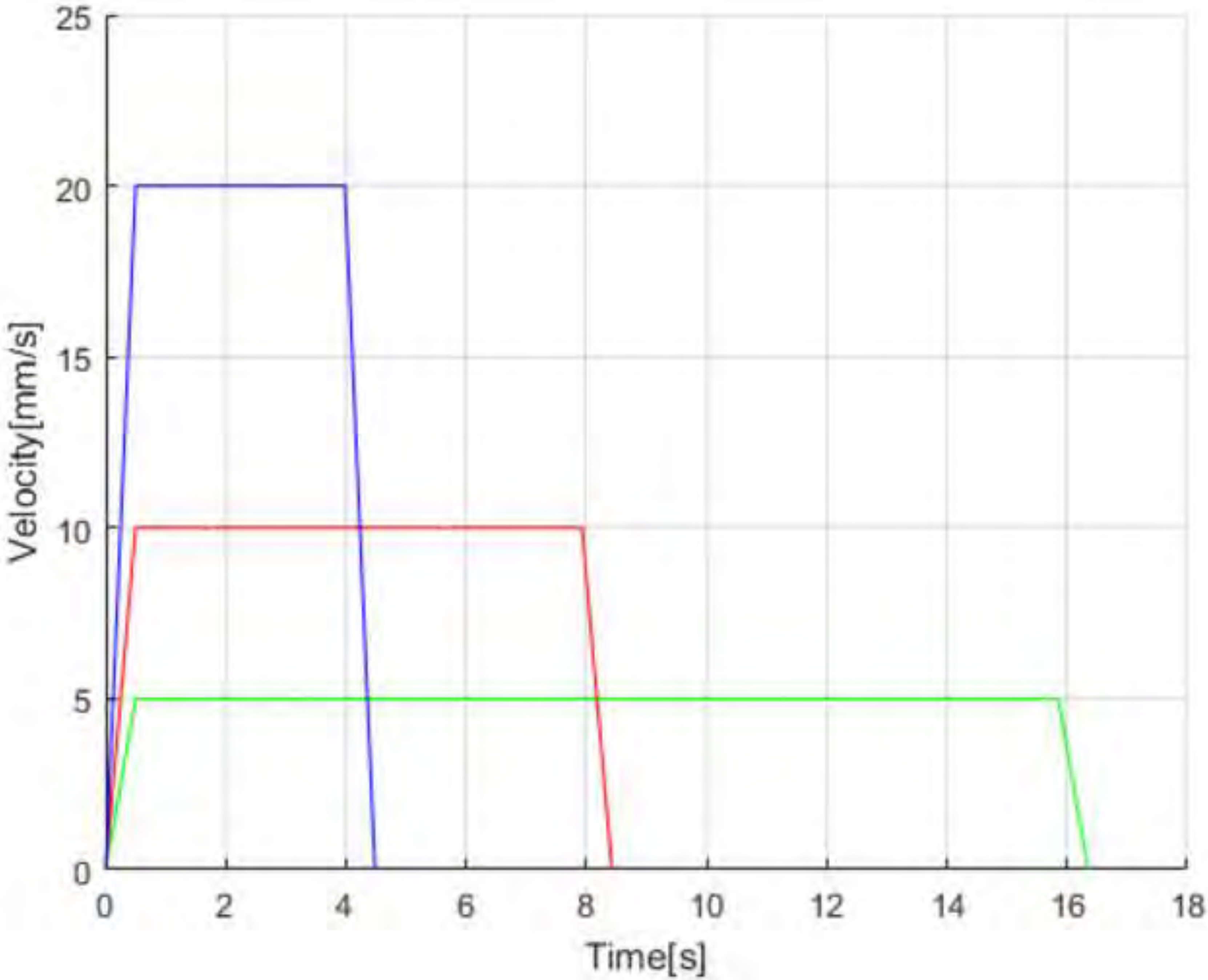

velocity2.png
Click here to download high resolution image